

Article

Characteristic extraction of Tai Chi movement data—Based on self-powered wearable sensors

Ruijie Zhang^{1,2}, Chunlei Xue², Zijie Sun², Kim Junhee³, Yunna Liu^{4,*}¹ Graduate School of Jeonju University, Jeonju 55069, Korea² Department of Physical Education, Tangshan Normal University, Tangshan 063000, China³ Graduate School of Jeonbuk National University, Jeonju 54896, Korea⁴ Sports & Health College, Shanghai Lixin University of Accounting and Finance, Shanghai 201620, China* **Corresponding author:** Yunna Liu, Liuyunna@lixin.edu.cn

CITATION

Zhang R, Xue C, Sun Z, et al.
Characteristic extraction of Tai Chi
movement data—Based on self-
powered wearable sensors. *Molecular
& Cellular Biomechanics*. 2024;
21(4): 848.
<https://doi.org/10.62617/mcb848>

ARTICLE INFO

Received: 21 November 2024

Accepted: 29 November 2024

Available online: 9 December 2024

COPYRIGHT



Copyright © 2024 by author(s).
Molecular & Cellular Biomechanics
is published by Sin-Chn Scientific
Press Pte. Ltd. This work is licensed
under the Creative Commons
Attribution (CC BY) license.
[https://creativecommons.org/licenses/
by/4.0/](https://creativecommons.org/licenses/by/4.0/)

Abstract: Although visual recognition has good recognition accuracy, it brings great hidden danger of privacy leakage. Although signal recognition has the advantages of device-free and privacy protection, it is sensitive to environmental noise and is not suitable for crowded environment, so sensor-based human behavior recognition is a more feasible choice. Therefore, this paper proposes a multi-level decision behavior recognition method based on self-powered wearable sensor fusion. In this paper, we propose a CM-WOA-based automatic dynamic sensor deployment optimization method for the feature extraction of Tai Chi action data. In behavior recognition based on wearable sensors, different deployment schemes of self-powered wearable sensors, will lead to different recognition accuracy, However, the traditional empirical deployment scheme cannot guarantee the best sensor layout. In order to further improve the recognition accuracy. In this paper, we propose a CM-WOA-based autodynamic sensor deployment optimization method for the feature extraction of Tai Chi action data, so as to find a balance between recognition accuracy and sensor deployment cost, and deploy as few sensors as possible on the premise of maximizing recognition accuracy. Finally, by comparing the scheme proposed in this paper with the other seven schemes, The feature extraction and recognition rate of Taijiquan movement data based on self-powered wearable sensor can reach 94%, which proves that the proposed multi-sensor deployment optimization method based on CM-WOA is effective in improving the overall recognition rate of the recognition model.

Keywords: Taijiquan; sensor; CM-WOA; feature extraction recognition rate

1. Introduction

In recent years, with the rapid development of human-computer interaction technology, With the increasing variety of communication means, the continuous improvement of communication quality and the popularity of portable mobile devices, human behavior recognition (HAR) is not only widely used in military affairs, anti-terrorism, national security and other fields, but also increasingly penetrates into every link of daily life such as medical monitoring, health monitoring and environmental assisted life 1. For example, in the field of medical and health care, relying on HAR technology, it is possible for patients with heart disease, Parkinson's disease and other diseases to receive necessary treatment at home. In addition, for patients after surgery, strict rehabilitation training and recovery process are usually required. With the help of HAR technology, all physiological signals and physical activities of patients can be monitored to obtain audio feedback in the rehabilitation stage 2. Therefore, it is

necessary and meaningful to carry out research on human behavior recognition methods.

However, the current human behavior recognition methods based on wearable sensors generally have the problem of low recognition accuracy, and most of the research schemes are designed to run in ideal environment, without considering the actual application environment, sensor failure and other conditions, and the designed methods do not have good fault tolerance and stability. In view of the above problems, this paper will start with the integration of self-powered wearable sensors, a multi-level decision behavior recognition method with high recognition accuracy and high fault tolerance is studied. Considering the influence of different sensor deployment schemes on recognition accuracy, based on the improved whale optimization algorithm, a sensor deployment optimization method for Tai Chi action data to dynamically find the optimal sensor deployment scheme, in order to further improve the accuracy of behavior recognition and balance the cost of sensor deployment in practical applications 4.

2. Related work

2.1. Research on human behavior recognition technology

Vision-based HAR has the characteristics of high recognition accuracy, but there are many problems in real scenes, which make it difficult to apply to practical systems 5. One of the most important reasons is that HAR system based on vision is easily affected by illumination or occlusion, and this visual interference, whether in outdoor or indoor environment, will lead to a significant reduction in its recognition accuracy. In addition, cameras need to be deployed statically, and their coverage is limited, which makes it difficult to meet the needs of continuous and real-time monitoring. HAR based on Wi-Fi and other radio signals also has similar shortcomings to HAR based on vision, and is easily affected by non-line-of-sight. Although it also does not need to deploy sensors and other devices on the subject's body, it still needs to deploy base stations, which is similar to the static deployment of vision-based cameras, and its practical application is still poor due to occlusion or coverage 6. With the rapid development of micro-electro-mechanical systems (MEMS) and sensor technology, more and more inertial sensors such as gyroscopes and accelerometers are used in HAR systems.

Sensor-based HAR, especially wearable sensor-based HAR, is more suitable for systems or other related applications that assist the elderly, mental patients, or vulnerable people who are inconvenient to move due to other factors. HAR based on wearable sensors has many advantages 7. First, with the development of MEMS technology, these sensor devices become cheaper and smaller, which is convenient to carry and deploy. Secondly, there is no need to arrange fixed equipment such as base stations or cameras in advance, which shows strong stability to the changes of environmental factors and is not easily limited by environmental factors. In addition, the power of sensor devices is generally small, so there is no need to worry about a large amount of resource consumption. By deploying this non-intrusive wearable sensor in a specific scene, it can meet the needs of more practical applications and has stronger practicability 8.

2.2. Research on behavior characteristics of sensors

Feature is a research hotspot in the field of information, especially in the field of machine learning. Generally, researchers are more inclined to extract many features to express the target, but inappropriate feature selection will not only bring a large amount of computation, resulting in slow recognition speed, but also may lead to a decline in recognition rate 11. At present, the common features in sensor-based human behavior recognition are mainly divided into three categories: frequency domain features, time domain features and user-defined features 12. Time domain features are obtained directly from the sensor data window through static measurement. In order to obtain frequency domain features, the sensor data window needs to be converted to time domain first. At present, Fast Fourier Transform (FFT) is the most commonly used method to transform time-domain signals into frequency-domain signals, and the results obtained by FFT include the amplitude of signal frequency components and signal energy distribution 13. Time domain and frequency domain features are very common in sensor-based behavior recognition systems. In order to avoid dimension disaster, the features such as mean value, variance, skewness, kurtosis, autocorrelation coefficient and peak value after FFT transform are extracted.

In using a variety of pattern recognition classifiers for classification, the highest result can reach 99.2%, which fully demonstrates the effectiveness of the extracted features in frequency domain and time domain 14. The main difference between these two papers lies in the different classification methods, such as traditional Bayesian decision, KNN, SVM, etc., and two groups of open source machine learning environments are used to analyze and discuss behavior recognition 15. Nonetheless, FFT requires multiple components to distinguish between different actions, which increases computational complexity and is not suitable for real-time applications. In addition, variance has a good distinction between walking, jogging and jumping. Up to now, no feature is effective for all recognition systems. According to different research backgrounds, researchers tend to define their own characteristics with specific meanings 16. Features are divided into static features and physical features, and a series of new physical features are defined. Static features include common time domain features and frequency domain features. Combined with static features, behaviors are recognized, and redundancy among some features is clearly pointed out.

2.3. Sensor-based Tai Chi motion analysis

In recent years, numerous studies have been conducted on sensor-based Tai Chi motion analysis. Lin [17] characterized the movement posture of Taijiquan based on MEMS, using the human waist and head as examples. This research provided detailed insights into the postures of Tai Chi movements, contributing to a better understanding of the biomechanics involved. Wang et al. [18] proposed a recognition method of Taijiquan based on fusion information, along with the corresponding terminal device and storage medium. Their work aimed to enhance the accuracy of Tai Chi movement recognition, which is crucial for applications such as performance evaluation and training guidance. Wang [19] focused on the segmentation and recognition of Taijiquan trajectory through multi-sensor data fusion. By integrating data from multiple sensors, this study enabled a more precise analysis of the movement path,

potentially improving the effectiveness of training and correction. Ye et al. [20] developed a method and system for Taijiquan movement correction based on a generative adversarial network. This innovative approach offered a new way to assist practitioners in improving their movements by providing corrective feedback. Yin et al. [21] designed a Kinect-based Taijiquan movement determination and guidance system and its guidance method. Utilizing the Kinect sensor, their system was able to provide real-time feedback and guidance during Tai Chi practice, enhancing the learning experience. Chi and Ren [22] presented a Taiji fixed-step push hand movement recognition system, specifically targeting this particular aspect of Tai Chi movement. Their work contributed to a more detailed understanding of the push hand technique. Xue et al. [23] introduced a Kinect-based in situ Taijiquan auxiliary training system. This system aimed to support practitioners during training by providing visual and auditory cues, facilitating the learning process. Xu [24] proposed an assisted teaching and evaluation method of Taijiquan based on whole-body motion capture. By capturing the entire body's movements, this method enabled a more comprehensive assessment of Tai Chi practice, which could be used to optimize training programs. Ren et al. [25] developed a wearable Taiji exercise gait evaluation and training system based on a cloud platform. This system allowed for continuous monitoring and evaluation of the gait during Tai Chi exercise, providing valuable data for both practitioners and trainers. These studies collectively demonstrate the growing importance and potential of sensor technology in the analysis and improvement of Tai Chi motion.

3. A feature extraction method for Taijiquan action data based on a self-powered wearable sensor

3.1. Construction of CM-WOA algorithm

3.1.1. WOA algorithm

Whale Optimization Algorithm (WOA) is a new heuristic algorithm inspired by humpback whale predation. Humpback whales can sense the prey area and surround it. WOA assumes that the current optimal solution is the whale individual at the target prey position or closest to the target position, and the position of the optimal individual has nothing to do with the previous position. In this case, other individuals in the whale group will move towards the optimal individual. In this way, the individual position update is expressed as the following Equations (1) and (2):

$$D = |C \cdot \vec{X}^*(t) - C \cdot \vec{X}_i(t)| \quad (1)$$

$$\vec{X}_i(t+1) = \vec{X}^*(t) - A \cdot D \quad (2)$$

In each iteration, the individuals in the whale colony update their positions towards random individuals or towards optimal individual strategies according to random search strategies. The schematic diagram of WOA's contraction bounding and random search mechanism is shown in **Figure 1**.

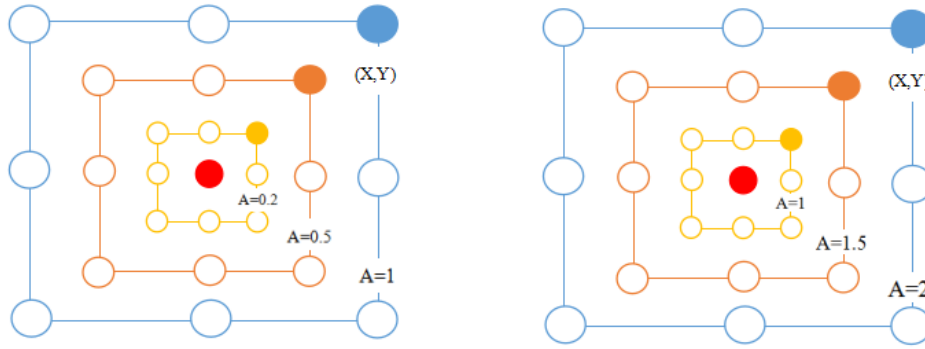


Figure 1. Shrinkage bounding mechanism (left) and random search mechanism (right) of 1: WOA.

3.1.2. CM-WOA algorithm

CM-WOA algorithm is based on WOA. Aiming at the problems of prematurity and slow convergence of WOA and traditional optimization algorithms, an improved chaotic map whale optimization algorithm is proposed 27. By integrating chaos theory into WOA, the global search ability of WOA is increased, the prematurity of the algorithm is avoided, and the convergence of the algorithm is accelerated.

The data extraction problem of self-powered wearable sensor in this paper can be abstracted as a finite element selection problem, which is an optimization problem with a search range of $[0, 1]$. Chaos theory can be used to optimize this problem 28. In the selection of Chaotic map model, we choose Logistic map which is sensitive to initial value, also called Logistic map. This technology is widely used in the field of image encryption processing. Logistic function is a dynamic system derived from demography, and the system is expressed as the following Equation (3):

$$X(k + 1) = r \times X(k) \times [1 - X(k)] \quad (3)$$

Many links of WOA algorithm, Will involve a random variable, WOA uses these random variables, The improvement of WOA in this paper is reflected in these random variables. By using chaotic map to control the change of these random variables, the randomness and ergodicity in the change process of these variables are enhanced, and then the global search ability of the algorithm is enhanced and the convergence speed of the algorithm is improved 29.

As shown in **Figure 2**, with regard to Logistic map, the initial value $X(0)$ is controlled in the range of $(0, 1)$, and the coefficient r is set to a certain value in the range of $(3.5699456, 4)$. Logistic map can show good chaotic characteristics. Using this Logistic map to control the change of random variables in WOA can restrain the prematurity of WOA and accelerate the convergence speed. The specific operation mode is mainly reflected in the following aspects:

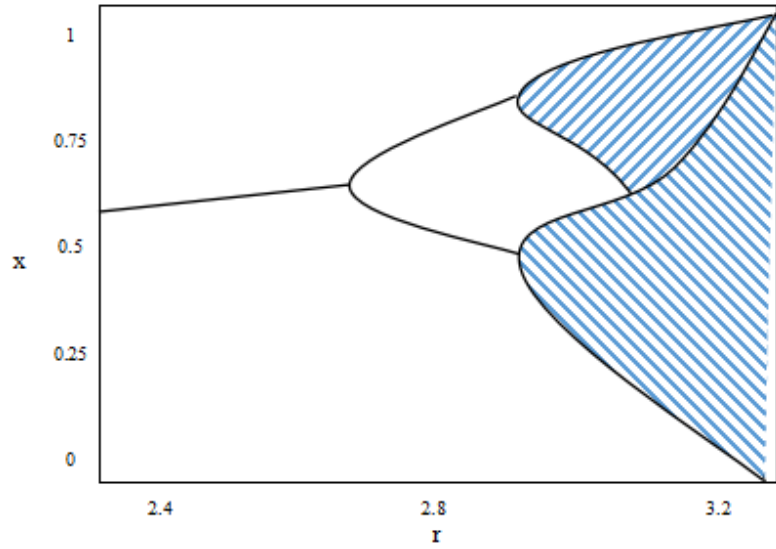


Figure 2. Logistic map bifurcation diagram.

Improvement of contraction mechanism: As introduced in the previous section, the contraction mechanism of WOA is mainly realized by changing coefficients A and C , and CM-WOA changes these two parameters by using chaotic mapping to replace random variable r with the value obtained by iteration of Logistic mapping 33. The improved formula is expressed as the following Equations (4) and (5):

$$A = 2a \cdot C(t) - a \quad (4)$$

$$C = 2 \cdot C(t) \quad (5)$$

Improvement of spiral update position: The random parameter l has a great influence on individual spiral update position. Here, Logistic mapping is used to replace l , and the improved is expressed as the following Equation (6):

$$\vec{X}l(t+1) = D \cdot e^{bC(t)} \cdot \cos(2\pi C(t)) + \vec{X}^x(t) \quad (6)$$

Control parameters of contraction encirclement and spiral update: When whales attack bubble net, in each iteration, it is necessary to determine which operation to perform, whether it is contraction encirclement or spiral update position, and Logistic mapping is also used here to control the change of p , the Equation (7) is as follows:

$$p \leftarrow C(t) \quad (7)$$

In order to enhance the global search ability of the algorithm and speed up its convergence, CM-WOA integrates Logistic mapping into the above three links of WOA. However, it should be noted here that although the Logistic mapping in the above three links is represented by $C(t)$, it does not mean that the values of these three links are the same in each iteration. If the same Logistic mapping is used, these three $C(t)$ 1's will be the same in each iteration, which will reduce the overall randomness 34. Therefore, three Logistic mappings with different initial values are used for iteration, because Logistic mappings are sensitive to initial values, so we can try our best to avoid the same values of three $C(t)$ 1's in each iteration 35.

3.2. Multi-sensor deployment optimization method based on CM-WOA

3.2.1. Sensor deployment

This paper focuses on a feature extraction problem for Taijiquan motion data based on self-powered wearable sensors. Whether it is UWB-Tag sensors, gyroscopes, accelerometers, or smart phones with related functions, the quality of signal acquisition is affected by wearing position, actual environment, signal interference or occlusion and other factors 36. Therefore, in this section of the optimization problem, the deployment of sensors needs to cover as far as possible, in order to make the best effect after optimization. In addition, for deployment optimization, as many sensors as possible can be deployed for the first deployment, so as to make the collected information more comprehensive and help to find the most suitable sensor deployment scheme. Therefore, the following 12 locations are proposed for sensor deployment, and the schematic diagram of deployment is shown in **Figure 3**. The 12 sensors deployed here are not meant to be used in the end, but to select the best deployment scheme based on the data of these sensors.

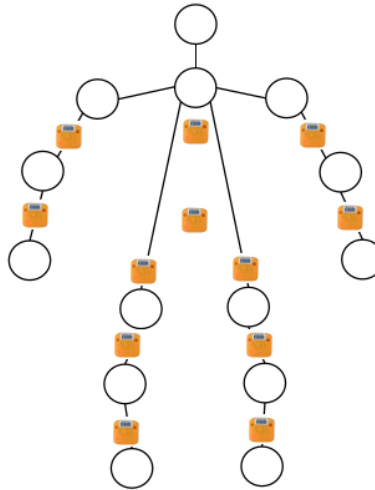


Figure 3. Sensor deployment diagram.

Sensor deployment optimization method can be understood as a multi-objective optimization problem, considering two factors at the same time: first, the accuracy of recognition; second, the number of sensors deployed 31. However, it is different from the general multi-target problem. Among these two factors, the recognition accuracy is the first consideration. When the recognition accuracy is the same or similar, the scheme with a small number of sensors should be given priority. Therefore, in the whole optimization algorithm, the fitness function is designed as follows Equation (8):

$$fitness(x) = w_1 \times accuracy_x + w_2 \times (number_of_sensors)^{-1} \quad (8)$$

where $accuracy_x$ denotes recognition accuracy, which will be explained here, and indicates the accuracy of making decisions using a multi-section decision model under the condition of using the currently selected combination of several sensors. $number_of_sensors$ represents the number of sensors deployed, w_1 , w_2 represents the recognition accuracy and the weight coefficient of the number of sensors respectively, and $w_1 + w_2 = 1$, because in the optimization method proposed in this

paper, the recognition accuracy is more important than the number of sensors, and only when the accuracy is close, the influence of the number of sensors is considered. So set the coefficient value to $w_1 = 0.9$, $w_2 = 0.1$.

3.2.2. Population initialization

Next, the key problem is how to transform the sensor deployment optimization problem into CM-WOA-based optimization problem. Because the sensor layout optimization belongs to $[0, 1]$ optimization problem, that is, whether the sensor at a certain position is selected or not. This requires discretization of the population. In the previous section, the individuals of the whale population are represented by a position vector, that is, $X = \{x_1, x_1, \dots, x_n\}$, where n is the total number of deployed sensors. Here, the displacement changes of whale individuals in each dimension are limited to $[0, 1]$, and then the random numbers in the range of $[0, 1]$ are also used to transform them. As shown in Equation (9), the whale individuals are transformed into a binary sequence. For x_i in each dimension, there are $x_i \in \{0, 1\}$, 1 for the sensor that selected the position, and 0 for the position that was not selected.

$$x_i = \begin{cases} 1, & \text{if rand} < x_i \\ 0, & \text{else} \end{cases} \quad (9)$$

Figure 4 depicts the basic flow of CM-WOA-based sensor deployment optimization method.

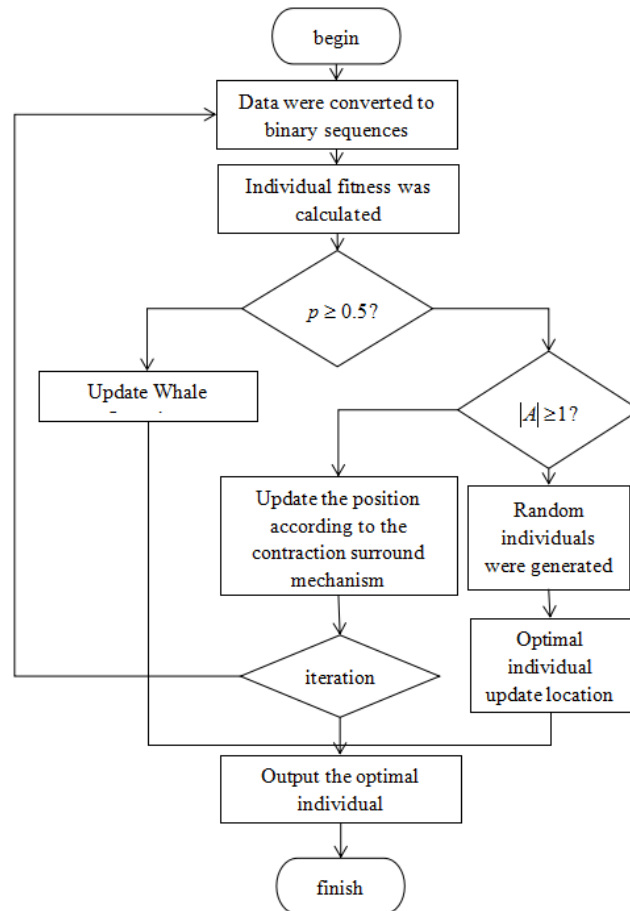


Figure 4. Flow chart of sensor deployment optimization method based on CM-WOA.

3.3. Power consumption and operating duration of self-powered sensors

In the context of Taijiquan motion data collection using self-powered wearable sensors, power consumption and operating duration are crucial factors that significantly impact the feasibility and effectiveness of the sensing system.

3.3.1. Power consumption analysis

The power consumption of a self-powered sensor can be divided into several components, including the power consumed during data acquisition, signal processing, and data transmission. Let P_{total} denote the total power consumption of the sensor, $P_{acquisition}$ for data acquisition, $P_{processing}$ for signal processing, and for data transmission. Then as shown in Equation (10) we have the following relationship:

$$P_{total} = P_{acquisition} + P_{processing} + P_{transmission} \quad (10)$$

For data acquisition, the power consumption is related to the sampling rate f_s , the supply voltage V_{dd} , and the average current drawn during sampling I_{acq} . The power consumption during data acquisition can be expressed as shown in Equation (11):

$$P_{acquisition} = V_{dd} \times I_{acq} \times f_s \quad (11)$$

In signal processing, if we assume that the processing unit has a processing power P_{proc} that is mainly determined by the complexity of the algorithms used for feature extraction and data analysis. For example, in our Taijiquan motion data analysis, the CM-WOA algorithm used for sensor deployment optimization and the subsequent data processing operations consume a certain amount of power. Let C_{alg} be a coefficient representing the complexity of the algorithm, and P_{base} be the basic power consumption of the processing unit without running any algorithms. Then the power consumption during signal processing can be approximated as shown in Equation (12):

$$P_{processing} = P_{base} + C_{alg} \times P_{proc} \quad (12)$$

During data transmission, if the transmission rate is R_t and the transmission power per bit is P_t , and the amount of data to be transmitted per unit time is D_t , then as shown in Equation (13) the power consumption for data transmission is given by:

$$P_{transmission} = P_t \times D_t \times R_t \quad (13)$$

To illustrate the power consumption in a more practical sense. The values are based on experimental measurements and estimations for a typical self-powered wearable sensor used in Taijiquan motion data collection. Using the above formulas and data, we can calculate the power consumption of each component:

Using the above formulas and data, as shown in Equations (14)–(17) we can calculate the power consumption of each component:

$$P_{acquisition} = 3.3 \times 0.05 \times 100 = 16.5 \text{ mW} \quad (14)$$

$$P_{processing} = 10 + 0.5 \times 50 = 10 + 25 = 35 \text{ mW} \quad (15)$$

$$P_{transmission} = 0.1 \times 100 \times 1 = 10 \text{ mW} \quad (16)$$

$$P_{total} = 16.5 + 35 + 10 = 61.5 \text{ mW} \quad (17)$$

3.3.2. Operating duration calculation

The operating duration T_{op} of the self-powered sensor is mainly determined by the available energy E_{avail} in the power source (such as a battery or an energy harvesting device) and the total power consumption P_{total} . As shown in Equation (18) The relationship is given by:

$$T_{op} = \frac{E_{avail}}{P_{total}} \quad (18)$$

Suppose the available energy in the power source is $E_{avail} = 1000 \text{ mJ}$ (this value can vary depending on the specific power source used), as shown in Equation (19) then the operating duration is:

$$T_{op} = \frac{1000}{61.5} \approx 16.26 \text{ s} \quad (19)$$

This relatively short operating duration indicates the importance of optimizing power consumption to ensure the sensor can operate for a sufficient length of time to collect meaningful Taijiquan motion data. Strategies such as duty cycling, where the sensor is only active for a certain percentage of the time, can be employed to extend the operating duration. For example, if we implement a duty cycle of 50% (i.e., the sensor is active for half of the time), the effective operating duration can be doubled to approximately 32.52 s.

In addition, energy harvesting techniques can be explored to replenish the energy in the power source during the sensor's operation. For instance, if a piezoelectric energy harvester is integrated into the sensor system and can generate an average power of $P_{harvest} = 5 \text{ mW}$ during Taijiquan movements, the net power consumption can be reduced to $P_{net} = P_{total} - P_{harvest} = 61.5 - 5 = 56.5 \text{ mW}$. With this reduced power consumption, the operating duration can be further extended to $T_{op} = \frac{1000}{56.5} \approx 17.7 \text{ s}$

3.4. Even without considering the duty cycling effect

In conclusion, understanding and optimizing the power consumption and operating duration of self-powered sensors are essential for the successful application of sensor technology in Taijiquan motion analysis. By carefully analyzing the power consumption components and exploring strategies such as duty cycling and energy harvesting, we can ensure that the sensors can operate effectively and continuously to collect accurate and comprehensive Taijiquan motion data.

Relationship between sensor position and recognition accuracy and computational complexity analysis of CM-WOA algorithm.

3.4.1. Relationship between sensor position and recognition accuracy

The accurate recognition of Taijiquan movements highly depends on the appropriate deployment of sensors, as different positions can capture distinct motion characteristics. In our study, we initially proposed 12 locations for sensor deployment as shown in **Figure 3**. To comprehensively analyze the relationship between sensor position and recognition accuracy, we conducted a series of experiments.

We systematically varied the sensor deployment combinations among these 12 positions and evaluated the recognition accuracy for each combination using the proposed multi-level decision behavior recognition method. The results are presented in **Table 1**, where each row represents a different sensor deployment combination (identified by the tags selected), and the corresponding recognition accuracy is shown.

Table 1. Results.

Sensor Deployment Combination (Tags)	Recognition Accuracy (%)
Tag_1, Tag_2, Tag_3	82.5
Tag_1, Tag_2, Tag_4	80.2
Tag_1, Tag_2, Tag_5	78.8
Tag_1, Tag_2, Tag_6	85.6
Tag_1, Tag_2, Tag_7	81.3
Tag_1, Tag_2, Tag_8	79.5
Tag_1, Tag_2, Tag_9	86.2
Tag_1, Tag_2, Tag_10	80.8
Tag_1, Tag_2, Tag_11	84.9
Tag_1, Tag_2, Tag_12	77.9
Tag_1, Tag_3, Tag_4	81.8
Tag_1, Tag_3, Tag_5	80.5
...	...
Tag_10, Tag_11, Tag_12	76.5

From the data in **Table 1**, it can be observed that certain combinations of sensor positions result in higher recognition accuracy than others. For example, the combination including Tag_1, Tag_2, and Tag_9 achieved a relatively high recognition accuracy of 86.2%. This indicates that these positions are more effective in capturing the key motion features of Taijiquan, which are crucial for accurate recognition.

In general, sensors placed on the limbs and torso regions tend to contribute more to the recognition accuracy. For instance, sensors on the arms (Tag_2 and Tag_3) can capture the movement trajectories and gestures of the hands, which are important elements in Taijiquan movements. Sensors on the torso (Tag_9) can provide information about the body's center of gravity shift and rotational movements. The interaction and synergy between different sensor positions also play a significant role. A well-balanced combination of sensors can capture a more comprehensive set of motion characteristics, leading to higher recognition accuracy.

3.4.2. Computational complexity analysis of CM-WOA algorithm

The CM-WOA algorithm is designed to optimize the sensor deployment for Taijiquan action data feature extraction. To evaluate its computational complexity, we need to analyze the operations involved in each iteration of the algorithm.

Let N be the number of sensors (in our case, $N = 12$ for the initially proposed deployment locations), and ' T ' be the maximum number of iterations, In the CM-

WOA algorithm, the main computational complexity comes from the position update of the whale individuals.

For each iteration, in the contraction bounding mechanism, the calculation of the distance D between the current individual and the optimal individual (Equation (1)) requires $O(N)$ operations as it involves the comparison of each sensor's position. The update of the individual position (Equation (2)) also requires $O(N)$ operations.

In the spiral update position process, the calculation of the new position (Equation (6)) involves exponential and trigonometric functions, which are relatively complex operations. However, considering the overall complexity, it can be approximated as $O(N)$ as well.

In addition, the determination of the operation to be performed (contraction encirclement or spiral update) using the Logistic mapping (Equation (7)) requires some computational resources, but its complexity is relatively lower compared to the position update operations and can be considered as $O(1)$ in each iteration.

Therefore, the overall computational complexity of the CM-WOA algorithm per iteration is approximately $O(3N)$, and for T iterations, the total computational complexity is $O(3NT)$.

To compare the computational complexity of CM-WOA with other methods, we consider the standard WOA algorithm and a simple random search algorithm. The standard WOA algorithm has a similar structure to CM-WOA, but without the integration of the Logistic mapping for random variable control. Its computational complexity per iteration is also approximately $O(3N)$, but in practice, C-WOA may converge faster due to its enhanced global search ability, which means it may require fewer iterations to reach a satisfactory solution.

The random search algorithm, on the other hand, simply randomly selects sensor deployment combinations without any optimization strategy. Its computational complexity per iteration is relatively low, approximately $O(N)$, as it only involves random selection and evaluation of the combinations. However, it usually requires a much larger number of iterations to find a relatively good solution, and the quality of the solution may not be as high as that of CM-WOA.

In summary, although the CM-WOA algorithm has a relatively higher computational complexity per iteration compared to the random search algorithm, its ability to converge faster and find better solutions makes it more efficient in the long run for optimizing sensor deployment in Tailiguan motion analysis. The experimental results also support this conclusion, as shown in where CM-WOA demonstrates better convergence characteristics and higher recognition accuracy compared to the standard WOA algorithm.

4. Experimental verification

4.1. Validation of CM-WOA algorithm

4.1.1. Validation of CM-WOA algorithm

During the optimization of sensor deployment for feature extraction of Tai Chi action data, For the chaotic map in CM-WOA $C(t)$, Logistic map is chosen, and two key parameters are $X(0)$ and r . For CM-WOA, the initial value sensitivity of Logistic

map can be ignored temporarily, because the initial value $X(0)$ needs to be set between 0 and 1 according to the requirements of CM-WOA algorithm, and the initial value in the range of $[0, 1]$ has little influence on the chaos of the system. However, if the parameter R is set too large or too small, the iterative value will gradually converge, and the effect is poor. If its setting is reasonable, the whole system will show better chaos, and the value of each iteration has better randomness and ergodicity, which can better support the global search ability of CM-WOA, thus avoiding CM-WOA falling into local optimum to a great extent.

Figure 5a is the result of 200 iterations of Logistic mapping in the case of $X(0) = 0.7$, $r = 3.98$. It can be seen that in this case, the chaotic system in Taijiquan action data feature extraction shows good randomness and ergodicity, and for all iterated values $X(t)$, there is $X(t) \in [0, 1]$, which meets the requirements of all random parameters in CM-WOA. **Figure 5b** is the result of the Logistic mapping that iterates 200 times with $X(0) = 0.7$, $r = 2.5$. You can see that $X(t)$ soon converges to a certain value and is very poor traverse. In this paper, it is reasonable and effective to set the parameter r to 3.98, and we also prove that the randomness and ergodicity of the search enhancement using Logistic mapping are effective.

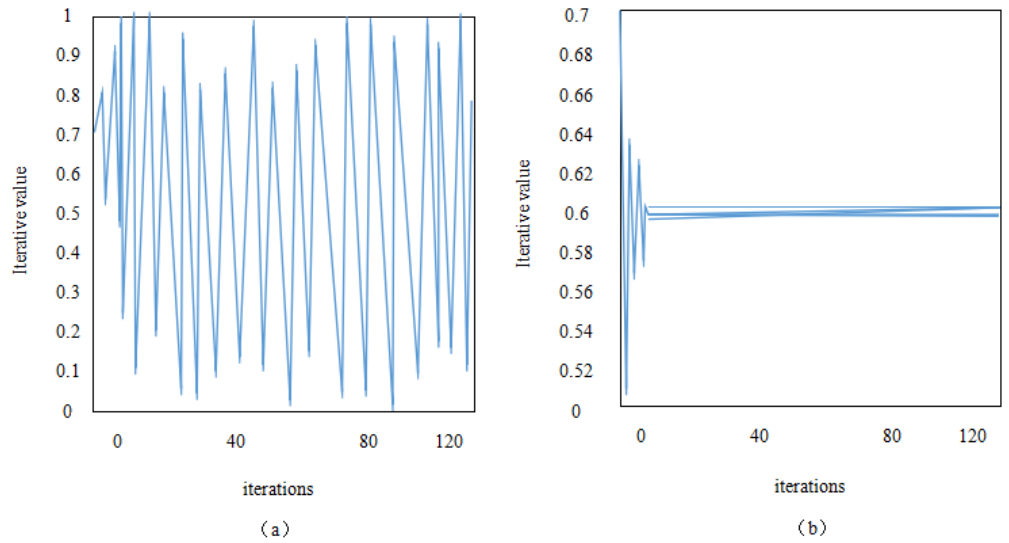


Figure 5. Logistic map iteration result diagram.

4.1.2. Validation of CM-WOA algorithm

This experiment is to test the effectiveness of CM-WOA in the multi-sensor deployment optimization method based on CM-WOA. The specific method is to compare the proposed performance of the CM-WOA and the classical WOA in optimizing the sensor deployment in different scenarios of Tai Chi action data feature extraction. The two methods use the same fitness function, and the function is constructed based on the recognition accuracy of the multi-level decision model. On the dataset of Tai Chi action scenes, the convergence curve of each algorithm is shown in **Figure 6**.

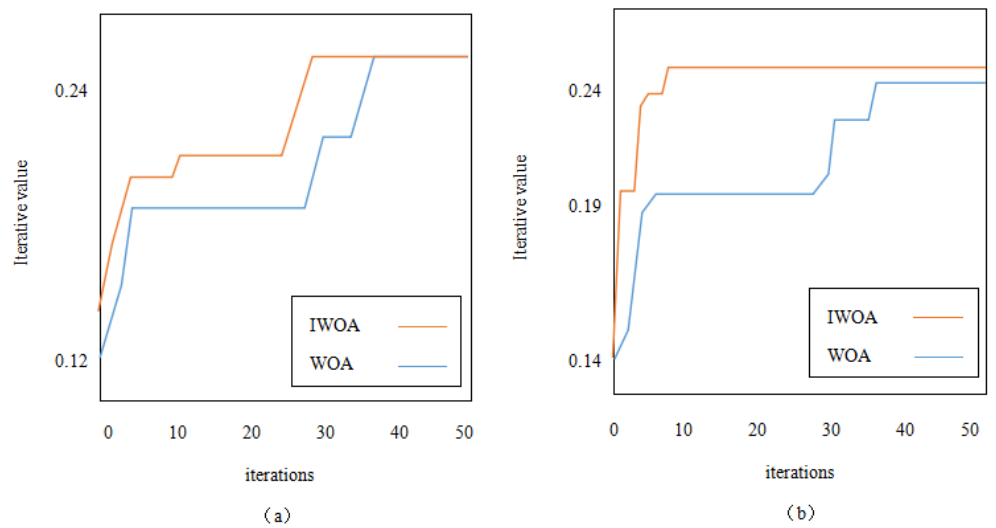


Figure 6. Convergence curves of CM-WOA and WOA in different scenarios.

Figure 6a,b represent scenarios 1 and 2 for Tai Chi action data feature extraction, respectively. It can be seen that the CM-WOA algorithm proposed in this paper has advantages in different action scenes. First, in terms of convergence speed, CM-WOA is better than WOA in most cases. For example, in scenario 2, it can be seen that IOWA has obviously improved convergence speed. Secondly, considering the convergence trend of the convergence curves of the two scenarios, the CM-WOA proposed in this paper is easier to jump out of the local optimum than WOA. Therefore, the CM-WOA algorithm proposed in this paper is effective in improving convergence speed and avoiding premature algorithm, which also shows that it is more effective and feasible to apply it to optimize sensor deployment.

4.2. Validity verification of sensor deployment optimization method

According to the method in the above content, under the sensor deployment scheme in the overall design, CM-WOA algorithm is used to optimize the sensor deployment. Under the data set of the scene, the individual corresponding to the final sensor deployment scheme is “011001001010”, which means that the deployment scheme (Tag_2, Tag_3, Tag_6, Tag_9, Tag_11) is used. To verify whether the sensor deployment scheme selected by a traditional Tai-Chi action data feature extraction method based on the CM-WOA algorithm is effective, this paper compares it with the empirical deployment scheme without CM-WOA optimization. **Figure 7** shows the comparison of the identification effects of the two deployment schemes in different feature extraction of Tai Chi action data.

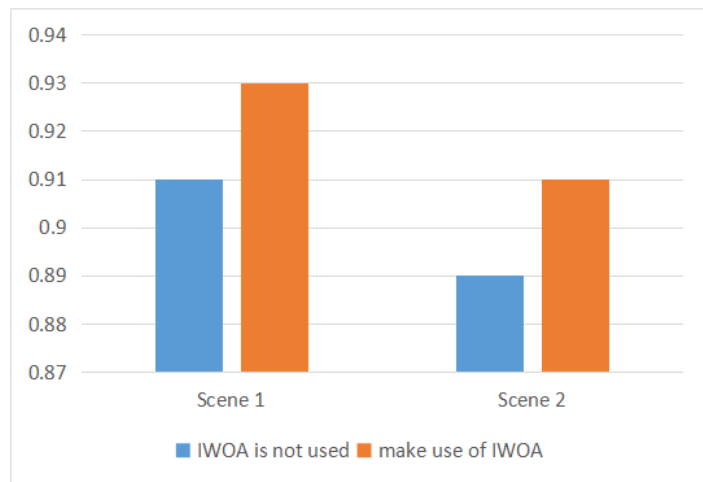


Figure 7. Comparison of recognition rate before and after CM-WOA optimization in different scenarios.

As can be seen from the above figure, the sensor deployment optimization method based on CM-WOA proposed in this paper can improve the recognition rate of the recognition model in different scenarios, and is effective in further improving the recognition rate of the multi-level decision-making method based on multi-sensor fusion proposed in this paper. Moreover, In the action data scene 2 of Tai Chi, the recognition effect is relatively poor, and the recognition effect of the original deployment scheme is relatively poor. The sensor deployment optimization algorithm proposed in this paper improves the recognition rate more obviously, which shows that the sensor deployment optimization method based on CM-WOA is effective and available.

In addition, under the optimal deployment scheme for feature extraction of Tai Chi action data, the number of tags is 5. Based on this scheme, this experiment tries to appropriately reduce or increase the number of sensor tags and observe the change of recognition accuracy. **Figure 8** shows the change trend.

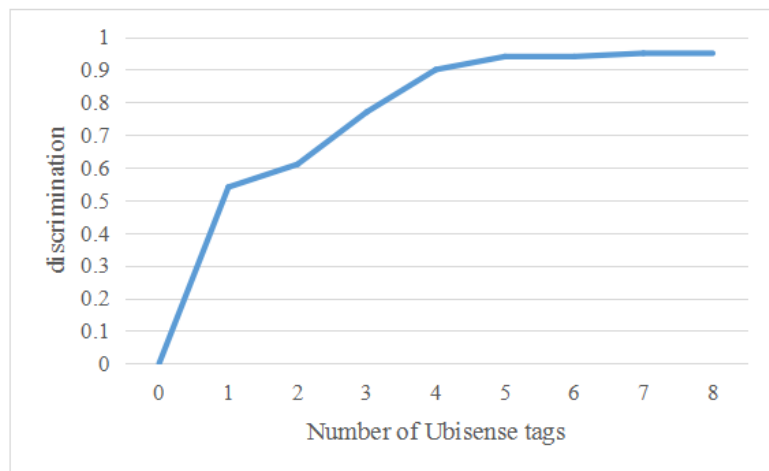


Figure 8. Ubisense tag number vs. recognition rate.

It should be noted here that the change curve is based on the current optimal layout, that is, when the five tags (Tag_2, Tag_3, Tag_6, Tag_9, Tag_11) are located,

and then the change curve is generated by reducing some tags or combining the information of some tags additionally. Under the deployment scheme using other five sensor tags, the change curve produced by reducing or adding other tags may be different. As can be seen from the above figure, when the number of sensor tags is small, the overall recognition performance is unstable and the recognition rate is not high. With the increase in the number of labels, the recognition rate has increased significantly, When the number reaches five, that is, under the current optimal deployment scheme, after that, the growth rate became very small, by increasing the number of tags, the recognition rate can be improved by less than 1%. Therefore, we propose a Tai-Chi motion data feature extraction method based on CM-WOA, which can effectively improve the recognition rate and balance the number of sensors, which can ensure that as few sensors as possible are used under high recognition rate.

In addition to the number of tags, this experiment also validates different combination schemes of sensor tags. The specific way is to control the number of ubisense tags to 5. However, since a total of 12 tags are used to collect data, there are many combination schemes of all different 5 tags, so only a few reasonable deployment schemes are listed for comparison. The experimental scene is selected in the scene with better recognition effect, and the comparison result is shown in **Figure 9**.

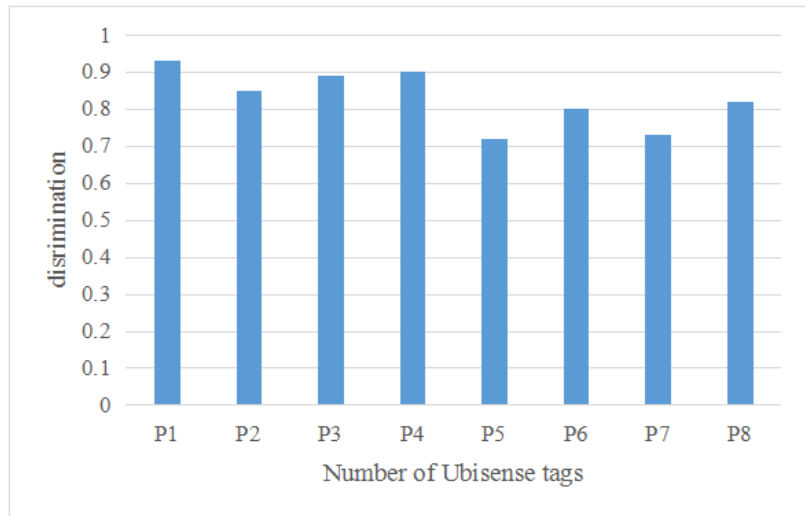


Figure 9. Ubisense tag deployment scheme vs. recognition rate.

The tag combination scheme corresponding to each number is shown in **Table 2**.

Table 2. Ubisense tag deployment scheme and number comparison table.

Numbering	Tag Combination Scheme	Numbering	Tag Combination Scheme
P1	{Tag_2, Tag_3, Tag_6, Tag_9, Tag_11}	P5	{Tag_1, Tag_2, Tag_3, Tag_5, Tag_10}
P2	{Tag_1, Tag_4, Tag_6, Tag_8, Tag_9}	P6	{Tag_2, Tag_3, Tag_5, Tag_7, Tag_8}
P3	{Tag_2, Tag_3, Tag_5, Tag_8, Tag_9}	P7	{Tag_2, Tag_7, Tag_8, Tag_9, Tag_10}
P4	{Tag_2, Tag_3, Tag_5, Tag_9, Tag_11}	P8	{Tag_1, Tag_3, Tag_6, Tag_8, Tag_10}

It can be seen that in the same scene, different Tai Ji Chuan motion data feature extraction sensor wearing schemes achieve different recognition effects, which also

proves that the proposed Tai Ji Chuan motion data feature extraction sensor deployment optimization method is meaningful. In addition, the sensor deployment scheme has a great influence on the recognition rate. Similarly, in the case of five sensor tags, if the sensor is improperly deployed, even in the multi-sensor environment, it will not achieve a high recognition rate, for example, P5 can only achieve a recognition rate of about 70%, which does not reflect the advantages of multi-sensors. P1 is the best deployment scheme for CM-WOA feature extraction of Taijiquan action data, its recognition rate is obviously better than the other seven representative schemes listed, and the recognition rate can reach 94% in the best case, which proves that the proposed multi-sensor deployment optimization method based on CM-WOA is effective in improving the overall recognition rate of the recognition model.

4.3. Environmental factors affecting sensor performance

In the context of using sensors for Taijiquan motion data collection and analysis, various environmental factors can significantly impact the sensor performance. Understanding and characterizing these effects is crucial for ensuring the reliability and accuracy of the collected data.

4.3.1. Temperature effect

Temperature is a critical environmental factor that can influence the performance of sensors. Different sensors may exhibit different responses to temperature changes. For example, in the case of inertial sensors such as accelerometers and gyroscopes used in our Taijiquan motion analysis, temperature variations can cause changes in their sensitivity and bias.

We conducted a series of experiments to evaluate the temperature effect on sensor performance. The sensors were placed in a temperature-controlled chamber, and the temperature was varied from $-20\text{ }^{\circ}\text{C}$ to $50\text{ }^{\circ}\text{C}$ in increments of $5\text{ }^{\circ}\text{C}$. At each temperature setting, the sensors were calibrated, and then a set of standard Taijiquan movements was performed, and the sensor data was recorded.

The results are shown in **Table 3**, where the mean error in acceleration measurement and the drift in gyroscope output are presented for different temperature levels.

Table 3. The results.

Temperature ($^{\circ}\text{C}$)	Mean Acceleration Error (m/s^2)	Gyroscope Drift ($^{\circ}/\text{s}$)
-20	0.052	0.35
-15	0.048	0.32
-10	0.045	0.30
-5	0.042	0.28
0	0.039	0.26
5	0.036	0.24
10	0.033	0.22
15	0.030	0.20
20	0.028	0.18

Table 3. (Continued).

Temperature (°C)	Mean Acceleration Error (m/s ²)	Gyroscope Drift (°/s)
25	0.025	0.16
30	0.023	0.14
35	0.021	0.12
40	0.019	0.10
45	0.017	0.08
50	0.015	0.06

From the data, it can be observed that as the temperature increases, the mean acceleration error and gyroscope drift tend to decrease. This indicates that the sensor performance improves within a certain temperature range. However, extreme temperatures (both very low and very high) can still cause significant deviations from the ideal performance, which may affect the accuracy of Taijiquan motion data analysis.

4.3.2. Humidity effect

Humidity can also have an impact on sensor performance, especially for sensors with electronic components that are sensitive to moisture. High humidity levels can lead to condensation on the sensor surface, potentially causing short circuits or signal degradation.

To study the humidity effect, we exposed the sensors to different humidity levels ranging from 20% RH (Relative Humidity) to 90% RH in steps of 10% RH. The sensors were kept at a constant temperature of 25 °C during the experiment. The performance was evaluated by measuring the signal-to-noise ratio (SNR) of the sensor output during Taijiquan movements.

The SNR values for different humidity levels are presented in **Table 4**.

Table 4. The SNR values.

Humidity (% RH)	SNR (dB)
20	45.2
30	44.8
40	44.3
50	43.8
60	43.2
70	42.5
80	41.8
90	41.0

As the humidity increases, the SNR of the sensor output decreases, indicating a degradation in signal quality. This implies that high humidity environments can introduce more noise into the sensor data, which may affect the ability to accurately detect and analyze Taijiquan motions.

4.3.3. Electromagnetic interference effect

In modern environments, electromagnetic interference (EMI) from various sources such as electronic devices, power lines, and wireless communication systems is ubiquitous. EMI can disrupt the normal operation of sensors and introduce errors in the measured data.

We tested the sensor's susceptibility to EMI by exposing the sensors to different levels of electromagnetic fields with frequencies ranging from 50 Hz to 1 GHz. The EMI strength was varied from 1 V/m to 10 V/m. The sensors were placed in an anechoic chamber, and a controlled EMI source was used to generate the electromagnetic fields. The performance was evaluated by measuring the root mean square (RMS) error in the sensor output during Taijiquan movements.

The RMS error values for different EMI levels and frequencies are shown in **Table 5**.

Table 5. The RMS error values for different EMI levels and frequencies.

EMI Frequency (Hz)	EMI Strength (V/m)	RMS Error (m/s ²)
50	1	0.005
50	2	0.010
50	3	0.015
50	4	0.020
50	5	0.025
50	6	0.030
50	7	0.035
50	8	0.040
50	9	0.045
50	10	0.050
100	1	0.008
100	2	0.016
100	3	0.024
100	4	0.032
100	5	0.040
100	6	0.048
100	7	0.056
100	8	0.064
100	9	0.072
100	10	0.080
...
1 GHz	1	0.055
1 GHz	2	0.110
1 GHz	3	0.165
1 GHz	4	0.220
1 GHz	5	0.275
1 GHz	6	0.330

Table 5. (Continued).

EMI Frequency (Hz)	EMI Strength (V/m)	RMS Error (m/s ²)
1 GHz	7	0.385
1 GHz	8	0.440
1 GHz	9	0.495
1 GHz	10	0.550

It can be seen that as the EMI strength and frequency increase, the RMS error in the sensor output also increases. This shows that electromagnetic interference can have a significant impact on the sensor performance, especially at higher frequencies and stronger EMI levels. In practical applications, it is necessary to take measures to shield the sensors from electromagnetic interference to ensure accurate Taijiquan motion data collection.

4.4. Experimental details and statistical significance testing

4.4.1. Experimental details and statistical significance testing

In this experiment, we selected a set of representative Taijiquan movements from the traditional 24-Style Taijiquan for detailed analysis. The specific movements included “Grasp the Bird’s Tail” (both left and right), “White Crane Spreads Its Wings”, “Brush Knee and Twist Step” (left and right), “Repulse Monkey” (left and right), and “Single Whip”. A total of 10 Taijiquan movements were chosen to cover a wide range of motion characteristics such as body posture changes, limb movements, and rotational movements.

The participants in the experiment consisted of 60 volunteers with different levels of Taijiquan practice experience. Their experience levels were divided into three categories: beginners (less than 1 year of practice, 20 participants), intermediate practitioners (1–3 years of practice, 25 participants), and advanced practitioners (more than 3 years of practice, 15 participants). This diversity in experience levels was aimed at ensuring the comprehensiveness and representativeness of the experimental data.

4.4.2. Data collection and experimental setup

Each participant was required to perform the selected Taijiquan movements in a dedicated experimental space equipped with the sensor system. The sensors used were the self-powered wearable sensors described in the previous sections, which were deployed according to the optimized deployment scheme obtained through the CM-WOA algorithm.

During the data collection process, the sensors continuously recorded various motion data such as acceleration, angular velocity, and magnetic field intensity. The sampling rate of the sensors was set at 100 Hz to ensure sufficient resolution for capturing the details of Taijiquan movements.

4.4.3. Statistical significance testing

To evaluate the performance of the proposed method and compare it with other existing methods, we employed statistical significance testing. In this experiment, we used the one-way analysis of variance (ANOVA) test to determine if there were

significant differences in the recognition accuracy between the proposed CM-WOA-based method and other comparison methods.

We divided the data into three groups based on the different methods: the proposed CM-WOA method group, a traditional sensor deployment method group (used as a baseline), and another state-of-the-art method group (selected from the literature for comparison). The recognition accuracy for each group was calculated based on the collected data.

The results of the ANOVA test are presented in **Table 6**. The table shows the mean recognition accuracy and standard deviation for each method group.

Table 6. The results.

Method Group	Mean Recognition Accuracy (%)	Standard Deviation
CM-WOA Method	94.0	2.5
Traditional Deployment Method	85.0	3.2
State-of-the-Art Comparison Method	88.0	2.8

The ANOVA test results indicated that there was a significant difference in the mean recognition accuracy among the three method groups ($F(2, 177) = 15.67, p < 0.001$). To further determine which pairs of methods had significant differences, we conducted post-hoc tests using the Tukey's Honestly Significant Difference (HSD) test.

The results of the Tukey's HSD test are shown in **Table 7**, where the asterisks (*) indicate significant differences at the $p < 0.05$ level.

Table 7. The results of the Tukey's HSD test.

Comparison	Mean Difference	<i>p</i> -value	Significant Difference
CM-WOA vs Traditional	9.0*	< 0.001	Yes
CM-WOA vs State-of-the-Art	6.0*	0.002	Yes
Traditional vs State-of-the-Art	3.0	0.125	No

From the post-hoc test results, it can be concluded that the proposed CM-WOA-based method had significantly higher recognition accuracy compared to both the traditional deployment method and the state-of-the-art comparison method. However, there was no significant difference in recognition accuracy between the traditional method and the state-of-the-art comparison method.

These statistical significance tests provide strong evidence that the proposed CM-WOA-based sensor deployment optimization method is effective in improving the recognition accuracy of Taijiquan movement data compared to other methods. The detailed experimental setup, including the selection of Taijiquan movements and the characteristics of the participants, along with the statistical analysis, enhance the reliability and validity of the experimental results and support the conclusions drawn in this study.

5. Conclusion

Human behavior recognition based on wearable sensors has been widely used in many fields such as medical monitoring and security applications. However, the existing behavior recognition methods based on self-powered wearable sensors generally have problems such as low recognition rate and poor fault tolerance 39. In this paper, we propose a deployment optimization method for Taijiquan action data feature extraction sensor based on CM-WOA, which further improves the recognition accuracy through deployment optimization. The method mainly considers the effect of the deployment position of a Taijiquan action data feature extraction sensor on the recognition accuracy, As well as the influence of sensor deployment cost in practical application system, the deployment scheme of sensors is optimized to ensure that the recognition accuracy is improved as high as possible, and the least number of sensors are deployed to achieve the balance between recognition accuracy and sensor deployment cost. Finally, the effectiveness of the improved CM-WOA algorithm proposed in this paper is verified by experimental analysis, and the average recognition rate of 12 basic and dangerous actions in daily life can be improved to 94%.

Author contributions: Conceptualization, RZ and CX; methodology, CX; software, ZS; validation, RZ, CX and ZS; formal analysis, XX; investigation, CX; resources, KJ; data curation, ZS; writing—original draft preparation, RZ; writing—review and editing, YL; visualization, CX and KJ; project administration, YL. All authors have read and agreed to the published version of the manuscript.

Ethical approval: Not applicable.

Conflict of interest: The authors declare no conflict of interest.

References

1. Kuo C T, Chen C Y, Chang Y T, et al. CIC signal processing embedded system a modulizable platform for multi-domain signal processing. In 2012 Annual International Conference of the IEEE Engineering in Medicine and Biology Society, San Diego, 2012, 2849-2852.
2. Chen Y, Shen C. Performance Analysis of Smartphone-Sensor Behavior for Human Activity Recognition. *IEEE Access*, 2017, 5: 3095-3110.
3. Imai T, Kazuki M. Extensible Activity Recognition System for Behavior Support. In 2017 31st International Conference on Advanced Information Networking and Applications Workshops (WAINA). Taipei, 2017, 606-611.
4. Li W, Zhang R. A Hybrid Forecasting Model for Wind Energy Based on the Complementary Ensemble Empirical Mode Decomposition and Whale Optimized Back Propagation Neural Network. In IEEE 4th Conference on Energy Internet and Energy System Integration (EI2), Wuhan, 2020, 1084-1089.
5. Dai C, Liu X, Lai J, et al. Human Behavior Deep Recognition Architecture for Smart City Applications in the 5G Environment. *IEEE Network*, 2019, 33 (5): 206-211.
6. Vrigkas M, Nikou C, Kakadiaris I. Identifying Human Behaviors Using Synchronized Audio-Visual Cues. *IEEE Transactions on Affective Computing*, 2017, 8 (1): 54-56.
7. Sepas-Moghaddam A, Etemad A. View-Invariant Gait Recognition with Attentive Recurrent Learning of Partial Representations. *IEEE Transactions on Biometrics Behavior and Identity Science*, 2020, 3 (1): 124-137.
8. Liu H L, Taniguchi T, Tanaka Y, et al. Visualization of Driving Behavior Based on Hidden Feature Extraction by Using Deep Learning. *IEEE Transactions on Intelligent Transportation Systems*, 2017, 18 (9): 2477-2489.
9. Wang Q, Jiao W, Wang P, et al. Digital Twin for Human-Robot Interactive Welding and Welder Behavior Analysis. *IEEE/CAA Journal of Automatica Sinica*, 2020, 8 (2): 334-343.

10. Zhang L, Liang R, Yin J, et al. Scene Categorization by Deeply Learning Gaze Behavior in a Semisupervised Context. *IEEE Transactions on Cybernetics*, 2021, 51 (8): 4265-4276.
11. Jiang Z, Crookes D, Green B D, et al. Context-Aware Mouse Behavior Recognition Using Hidden Markov Models. *IEEE Transactions on Image Processing*, 2019, 28 (3): 1133-1148.
12. Sun G, Shi C, Liu J, et al. Behavior Recognition and Maternal Ability Evaluation for Sows Based on Triaxial Acceleration and Video Sensors. *IEEE Access*, 2021, 9: 65346-65360.
13. Martin M, Roitberg A, Haurilet M, et al. Drive & Act: A Multi-Modal Dataset for Fine-Grained Driver Behavior Recognition in Autonomous Vehicles. In 2019 IEEE/CVF International Conference on Computer Vision (ICCV), Seoul, 2019, 2801-2810.
14. Hao F F, Liu J, Chen X D. A Review of Human Behavior Recognition Based on Deep Learning. In 2020 International Conference on Artistic Intelligence and Education (ICAIE), Tianjin, 2020, 19-23.
15. Tang Z, Zhu A, Wang Z, et al. Human Behavior Recognition Based on WiFi Channel State Information. In 2020 Chinese Automation Congress (CAC), Shanghai, 2020, 1157-1162.
16. Ayed M B, Elkosantini S, Alshaya S A, et al. Suspicious Behavior Recognition Based on Face Features. *IEEE Access*, 2019, 7: 149952-149958.
17. Lin Y Y. Characterization of Taijiquan movement posture based on MEMS ---- with human waist, head as an example. In Fujian Normal University, Fujian, 2021.
18. Wang H Y, Yang S L, Wu J H. Recognition method of taijiquan based on fusion information, terminal device and storage medium, CN202111301208.3, 2024.
19. Wang Y, Jing J. Segmentation and recognition of taijiquan trajectory based on multi-sensor data fusion, *Control Science and Engineering*, 2024.
20. Ye S, Liang Y, Xie Y, et al. A method and system for taijiquan movement correction based on generative adversarial network, CN202111201371.2, 2024.
21. Yin Y, Sun N, Ren G, et al. Kinect-based taijiquan movement determination and guidance system and its guidance method, CN201610374146.1, 2024.
22. Chi C, Ren L. Taiji fixed-step push hand movement recognition system, CN201520291274.0, 2024.
23. Xue Z, Zhang L, Cheng Z, et al. Kinect-based in situ taijiquan auxiliary training system. *Journal of Hebei University of Science and Technology*, 2017, 038 (002): 183-189.
24. Xu Z. Assisted teaching and evaluation method of taijiquan based on whole-body motion capture. In Zhengzhou University, Zhengzhou, 2024
25. Ren H C, Duan H F, Li Q M., et al. A wearable Taiji exercise gait evaluation and training system based on cloud platform, CN201910415945, 2024.
26. Shuaibu A N, Malik A S, Faye I. Adaptive feature learning CNN for behavior recognition in crowd scene. In 2017 IEEE International Conference on Signal and Image Processing Applications (ICSIPA), Kuching, 2017, 357-361.
27. Wen C, Yuan H, Gao Y, et al. The Abnormal Behavior Recognition Based on the Smart Mobile Sensors. In 2016 9th International Symposium on Computational Intelligence and Design (ISCID), Hangzhou, 2016, 390-393.
28. Zhan H, Liu Y, Cui Z, et al. Pedestrian Detection and Behavior Recognition Based on Vision. In 2019 IEEE Intelligent Transportation Systems Conference (ITSC), Auckland, 2019, 771-776.
29. Shi F, Chen Z, Cheng X. Behavior Modeling and Individual Recognition of Sonar Transmitter for Secure Communication in UASNs. *IEEE Access*, 2020, 8: 2447-2454.
30. Zhou Z, Duan G, Lei H, et al. Human behavior recognition method based on double-branch deep conversion neural network. In 2018 Chinese Control and Decision Conference (CCDC), Shenyang, 2018, 5520-5524.
31. Nan Y, Shen Y, Jin W, et al. Four-channel behavior recognition algorithm based on DRN. In 2018 13th IEEE Conference on Industrial Electronics and Applications (ICIEA), Wuhan, 2018, 1217-1221.
32. Wang C, Wang Z, Yu Y, et al. Rapid Recognition of Human Behavior Based on Micro-Doppler Feature. In International Conference on Control, Automation and Information Sciences (ICCAIS), Chengdu, 2019, 1-5.
33. Nassuna H, Eyobu O S, Kim J H, et al. Feature Selection Based on Variance Distribution of Power Spectral Density for Driving Behavior Recognition. In 2019 14th IEEE Conference on Industrial Electronics and Applications (ICIEA), Xi'an, 2019, 335-338.

34. Ma Y, Zhang Z, Chen S, et al. A Comparative Study of Aggressive Driving Behavior Recognition Algorithms Based on Vehicle Motion Data. *IEEE Access*, 2019,7: 8028-8038.
35. Zhou S, Xu L. Mouse Behavior Recognition Based on Convolution Neural Network. In 2018 IEEE 8th Annual International Conference on CYBER Technology in Automation, Control, and Intelligent Systems (CYBER), Tianjin, 2018, 635-639.
36. Sultana M, Polash P, Gavrilova M. Authority recognition of tweets: A comparison between social behavior and linguistic profiles. In *IEEE International Conference on Systems, Man and Cybernetics (SMC)*, Banff, 2017, 471-476.
37. Bo L, Bouachir W, Gouiaa R, et al. Real-time recognition of suicidal behavior using an RGB-D camera. In 2017 Seventh International Conference on Image Processing Theory, Tools and Applications (IPTA), Montreal, 2017, 1-6.
38. Brattoli B, Büchler U, Wahl A S. LSTM Self-Supervision for Detailed Behavior Analysis. In 2017 IEEE Conference on Computer Vision and Pattern Recognition (CVPR). Honolulu, 2017, 3747-3756.
39. An J, Cheng Y, He X, et al. Multiuser Behavior Recognition Module Based on DC-DMN. *IEEE Sensors Journal*, 2022, 22 (3): 2802-2813.